The role of receptor internalization in CD95 signaling

**Kyeong-Hee Lee[1,4], Christine Feig[2,4],
Vladimir Tchikov[3,4], Robert Schickel[2],
Cora Hallas[3], Stefan Schütze[3],
Marcus E Peter[2,5] and Andrew C Chan[1,5,]***

[1]Department of Immunology, Genentech Inc., South San Francisco, CA, USA, [2]The Ben May Institute for Cancer Research, University of Chicago, Chicago, IL, USA and [3]Institute of Immunology, University Hospital of Schleswig-Holstein, Campus Kiel, Kiel, Germany

Activation of the cell surface CD95 receptor triggers a cascade of signaling events, including assembly of the death-inducing signaling complex (DISC), that culminate in cellular apoptosis. In this study, we demonstrate a general requirement of receptor internalization for CD95 ligand-mediated DISC amplification, caspase activation and apoptosis in type I cells. Recruitment of DISC components to the activated receptor predominantly occurs after the receptor has moved into an endosomal compartment and blockade of CD95 internalization impairs DISC formation and apoptosis. In contrast, CD95 ligand stimulation of cells unable to internalize CD95 results in activation of proliferative Erk and NF-κB signaling pathways. Hence, the subcellular localization and internalization pathways of CD95 play important roles in controlling activation of distinct signaling cascades to determine divergent cellular fates.

Introduction

Surface receptors transduce signals derived from the extracellular milieu to evoke a diverse range of cellular responses. This process is initiated upon ligand binding and transduced through the spatial and temporal regulation of physical interactions of receptors with intracellular signaling molecules. Gain- or loss-of function mutants alter the normal balance of cellular homeostasis that, in turn, can induce oncogenesis and/or developmental arrest. For many receptors, triggering by ligand results in receptor clustering that is followed by downregulation of activated surface receptors through endocytosis and subsequent lysosomal degradation (Ceresa and Schmid, 2000). These latter steps typically

*Corresponding author. Department of Immunology, Genentech Inc., MS-34, Bldg. 12-281, 1 DNA Way, South San Francisco, CA 94080, USA. Tel.: + 1 650 225 8104; Fax: + 1 650 225 8136; E-mail: acc@gene.com or MPeter@uchicago.edu
[4]These authors contributed equally to this work
[5]These authors shared senior authorship

attenuate signaling via removal of activated receptor complexes. Recent studies, however, indicate that receptor internalization can target activated receptors to the endocytic compartment, and contributes to both the intensity of signaling and assembly of signaling complexes (Miaczynska *et al*, 2004b).

CD95 (CD95/APO-1/TNFRSF6) is a prototypic death receptor belonging to the tumor necrosis factor (TNF) receptor superfamily (Li-Weber and Krammer, 2003). Interactions of CD95 with its ligand, CD95L (CD178/FasL/TNSF6), play a pivotal role in the regulation of peripheral tolerance and lymphoid homeostasis. Natural mutations within CD95 and CD95L in humans and mice are associated with the development of autoimmune lymphoproliferative syndromes (Nagata, 1999). CD95 is expressed on the surface of cells as preassociated homotrimers and, upon CD95L binding, undergoes a conformational change to reveal its cytoplasmic death domain (DD) to favor homotypic interactions with other DD-containing proteins (Itoh and Nagata, 1993; Boldin *et al*, 1995; Chinnaiyan *et al*, 1995; Siegel *et al*, 2000). Additional interactions mediated through the N-terminal 'death effector domain' (DED) of FADD with DED domains encoded within procaspase-8 and -10 assemble the death-inducing signaling complex (DISC) (Peter and Krammer, 2003). Efficient DISC assembly provides a molecular scaffold concentrating cysteine proteases to induce autoproteolytic cleavage of caspase-8 and, in turn, subsequent activation of the apoptotic pathway.

CD95-mediated apoptosis is transduced through two general modes (Algeciras-Schimnich *et al*, 2003; Barnhart *et al*, 2003). Type I cells exhibit rapid receptor internalization and form large amounts of DISC, while type II cells are more dependent upon the mitochondrial amplification pathway and exhibit quantitatively less and slower DISC assembly. We demonstrate here that CD95 internalization in type I cells plays a previously unrecognized requisite role in CD95L-induced activation of apoptotic pathways. In contrast, engagement of CD95 without receptor internalization results in activation of nonapoptotic signaling pathways. Hence, the subcellular compartment of CD95 signaling activates divergent biochemical pathways to promote distinct survival or apoptotic cellular fates.

Results

Expression of a plasma membrane localized PIP$_2$-specific 5-phosphatase modulates PIP$_2$ levels and inhibits CD95L-induced CD95 internalization and apoptosis

We have previously demonstrated that disruption of filamentous actin inhibits CD95 internalization, a process that normally proceeds through a clathrin-mediated endocytic compartment, and renders cells more resistant to CD95-mediated apoptosis (Algeciras-Schimnich *et al*, 2002; Algeciras-Schimnich and Peter, 2003). As cellular levels of

PIP$_2$ (PtdIns(4,5)P$_2$) have been shown to regulate clathrin-mediated endocytosis (Martin, 2001), we employed an enzymatic approach using the *Saccharomyces cerevisiae Inp54* 5-phosphatase (INP54p) that hydrolyzes PIP$_2$ to PI(4)P (Stolz *et al*, 1998). Targeting of a green fluorescent protein (GFP)–INP54p fusion protein to the plasma membrane (PM) was achieved by attaching a myristoylation/palmitoylation sequence from the Fyn protein tyrosine kinase (Shenoy-Scaria *et al*, 1993; Raucher *et al*, 2000) (Supplementary Figure 1A, middle panels). Expression of FynC-GFP-INP54p reduced PIP$_2$ levels in >98% of transfected GFP$^+$, but not of GFP$^-$, cells (Supplementary Figure 1B, middle panel). In contrast, expression of a mutant in which Cys 3 and 6, important for palmitoylation and PM localization, were mutated to Ser (designated as FynS-GFP-INP54p) resulted in a cytoplasmic distribution (Supplementary Figure 1A, right panels) and lesser effects on PIP$_2$ levels (Supplementary Figure 1B, bottom panel). PIP$_2$ levels were unaffected in cells expressing a control FynC-GFP cDNA (top panel).

We next investigated the functional consequences of reduced PIP$_2$ in CD95 function. BJAB cells, transiently transfected with FynC-GFP-INP54p, FynS-GFP-INP54p or FynC-GFP, were stimulated with Flag-tagged (Flag-)CD95L (SuperFasL, Apotech) and the degree of apoptosis was assessed by TUNEL staining. In FynC-GFP$^+$ or FynS-GFP-INP54p$^+$ cells, ∼65% of cells were TUNEL$^+$ following CD95L stimulation (Supplementary Figure 1C, left and right panels). In contrast, <5% of FynC-GFP-INP54p$^+$ BJAB cells were TUNEL$^+$ in response to CD95L treatment (middle panel). Inhibition of CD95L-induced apoptosis was observed at 5, 16, 24 and 48 h (Supplementary Figure 1D). Similar inhibition of CD95L-induced apoptosis was also observed in type I SKW6.4 cells (Supplementary Figure 2A). In contrast, expression of FynC-GFP-INP54p did not affect CD95L-mediated apoptosis in type II Jurkat T cells (Supplementary Figure 2B). FynC-GFP-INP54p expression did not induce a general defect in the apoptotic machinery in BJAB cells, as etoposide-induced apoptosis, which acts through a mitochondria-mediated intrinsic pathway (Shimizu *et al*, 1996), was unaffected (Supplementary Figure 2C). In addition, apoptosis-resistant FynC-GFP-INP54p$^+$ cells, following CD95L activation, retained normal cellular growth and were grossly indistinguishable from normal BJAB cells (data not shown).

To define the biochemical basis by which the CD95-mediated apoptosis was affected by FynC-GFP-INP54p, BJAB cells were stimulated with Flag-CD95L and activation of caspase-8 and -3 measured by immunoblotting for their self-cleavage products. While treatment of BJAB cells with Flag-CD95L resulted in a time dependent cleavage of both caspases (Figure 1A, lanes 1–4), no evidence for caspase-8 or -3 activation was detected in FynC-GFP-INP54p$^+$ BJAB cells (lanes 5–8). We next analyzed the recruitment of FADD to activated CD95, one of the most proximal biochemical events in DISC formation. While FADD readily co-immunoprecipitated with CD95L-bound CD95 in control cells, no association of FADD with activated CD95 was detected in FynC-GFP-INP54p$^+$ BJAB cells (Figure 1B, top row). Similarly, while caspase-8 and -10 were readily co-immunoprecipitated with CD95/CD95L complexes in control cells, neither was detected with activated CD95 in FynC-INP54p$^+$ BJAB cells (second and third rows). Taken together, these observations indicate that FynC-GFP-INP54p reduces cellular PIP$_2$ levels as well as

CD95L-induced FADD association with activated CD95, caspase activation and apoptosis.

As CD95L binding to CD95 was not altered by FynC-GFP-INP54p (Supplementary Figure 3A), we assessed the effects of FynC-GFP-INP54p on CD95 clustering. Cells were incubated with Flag-CD95L at 4°C, activation was induced by incubation at 37°C, and localization of CD95 analyzed by deconvolution microscopy. In wt BJAB cells (GFP$^-$ cells), CD95L induced small 'patch-like' receptor clusters at the PM within 5 min after stimulation (Figure 1C, panels 4–6, left cell). Expression of FynC-GFP-INP54p did not affect the ability of CD95L to induce CD95 clustering at the PM 5 min following activation (Figure 1C, panels 4–6, GFP$^+$ cells). By 15 and 30 min, the clustered CD95 in GFP$^-$ cells had internalized to intracellular compartments (Figure 1C, panels 7–12, left cell). In contrast, CD95 remained clustered at the PM for at least 30 min in FynC-GFP-INP54p$^+$ cells without any significant internalization following CD95L stimulation (Figure 1C, panels 7–12, right cell).

These results were further supported by flow-cytometric studies. In BJAB cells transfected with control FynC-GFP, CD95 downregulation was detected within 15 min following CD95L activation (Figure 1D, top panel). In contrast, FynC-GFP-INP54p$^+$ cells were unable to downregulate surface CD95 even 30 min following CD95L activation (bottom panel). Similar results were found for SKW6.4 cells (Supplementary Figure 2D).

Membrane-bound CD95L (mCD95L)-induced apoptosis requires CD95 internalization

Our data so far suggested that CD95-mediated apoptosis in response to a soluble form of CD95L (sCD95L) stimulation requires receptor internalization. However, it is widely assumed that the physiologic stimulus for CD95 is more likely to be mCD95L. We therefore incubated murine CT26 cells expressing human mCD95L (CT26mCD95L) with SKW6.4 cells. No soluble CD95L could be detected in CT26mCD95L cells or concentrated supernatant derived from cultures of these cells (Supplementary Figure 4B and data not shown). In SKW6.4 cells, CD95 was efficiently internalized when co-incubated with CT26mCD95L, but not in untreated SKW6.4 cells (Figure 2A and Supplementary Figure 4A and B). Correspondingly, CT26mCD95L cells induced a time-dependent processing of procaspase-8 (Supplementary Figure 4C). When SKW6.4 cells were overlaid on adherent CT26 cells, CD95 internalized in SKW6.4 cells contacting CT26mCD95L, but not control CT26, cells (Figure 2B, bottom panels). These data suggest that mCD95L induces internalization of CD95 as much as sCD95L.

We have previously shown that unmodified sCD95L does not induce CD95 apoptosis in type I cells (Algeciras-Schimnich *et al*, 2003). However, to exclude that the internalization and apoptosis observed in cells exposed to mCD95L were not due to very small amounts of secreted sCD95L, we expressed a mutant form of human mCD95L (designated as DA4) that cannot be cleaved from the membrane surface (Tanaka *et al*, 1998) on the surface of chicken DT40 B cells (Supplementary Figure 3B). Deconvolution microscopy confirmed that CD95 internalized into the cytoplasmic compartment when incubated with mCD95L(DA4)-expressing DT40 cells (Figure 2C, right panel), but not when incubated with control DT40 cells (left panel).
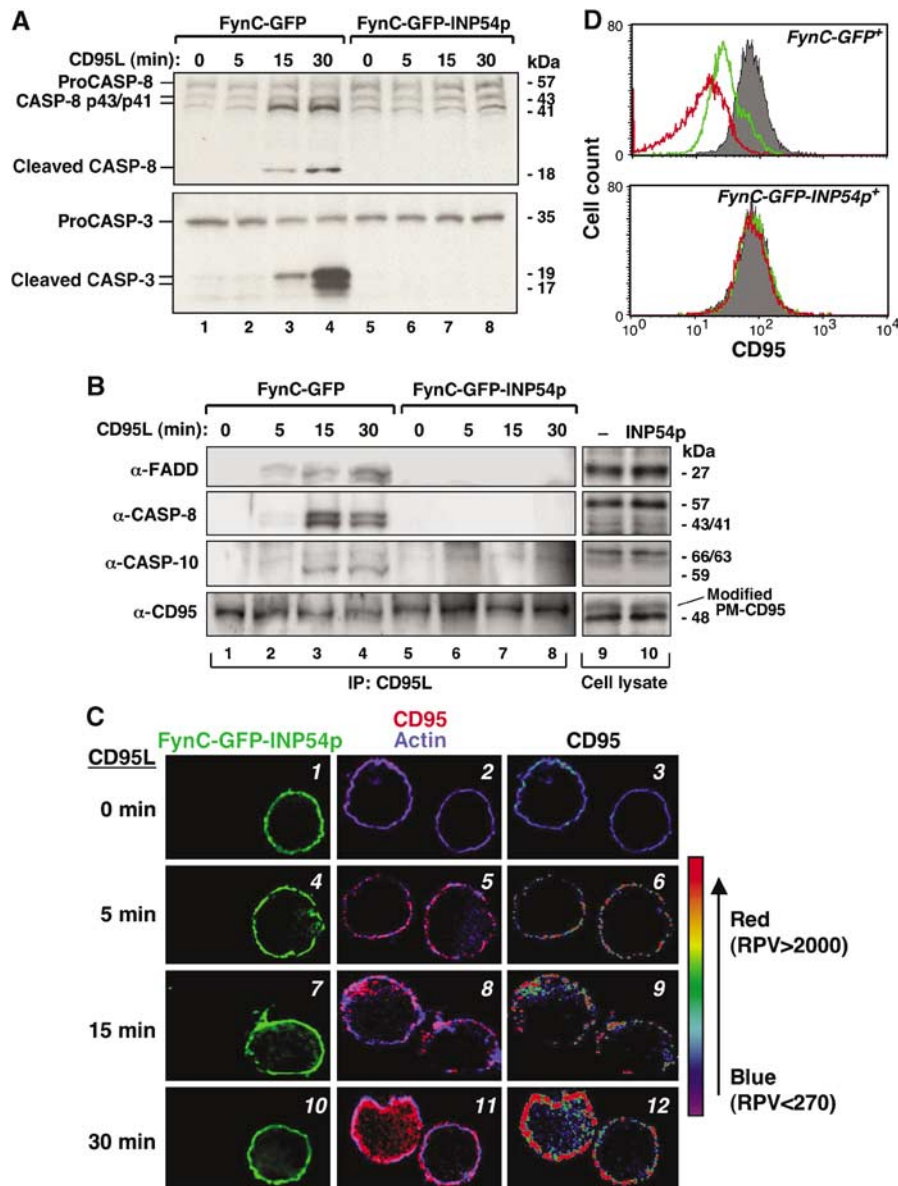
Figure 1 Defective CD95 internalization and apoptosis induction in FynC-GFP-INP54p-expressing cells. (**A**) Defective caspase activation in PM-targeted INP54p-expressing cells. BJAB cells expressing a control vector (lanes 1–4) or FynC-GFP-INP54p (lanes 5–8) were stimulated with Flag lanes-CD95L for the indicated times. Cells were lysed and analyzed for caspase-8 (top) and -3 (bottom) cleavage. Transfection efficiency was >90% using a dual-transfection protocol. Data shown are representative of two experiments. (**B**) Defective DISC assembly in PM-targeted INP54p-expressing cells. BJAB cells were treated as described in (A). CD95L–CD95 complexes were immunoprecipitated by use of anti-Flag Ab-coupled beads and analyzed for associated DISC proteins (lanes 1–8). Cell lysates were also analyzed for DISC proteins and CD95 expression (lanes 9 and 10). Data shown are representative of three experiments. (**C**) BJAB cells transiently transfected with FynC-GFP-INP54p were stimulated with Flag-CD95L for the indicated times. Permeabilized cells were visualized by deconvolution microscopy for GFP (green) in the left panels and stained for CD95 (red) and F-actin (blue) in the middle panels. Quantitative image analysis with RPVs recorded for CD95 fluorescence signals is shown in the right panels. Red indicates the highest and blue represents the lowest fluorescence intensity. RPV = relative pixel value. Data shown are representative of >150 cells analyzed. (**D**) Inhibition of CD95 internalization by FynC-GFP-INP54p. BJAB cells, transfected with FynC-GFP (top) or FynC-GFP-INP54p (bottom), were incubated with Flag-CD95L at 37°C for 15 (green) or 30 mins (red). As a control, cells were incubated with Flag-CD95L on ice (0 min, black). The remaining surface CD95 was detected by staining with an anti-CD95 mAb (DX2) and analyzed by flow cytometry. Data shown are representative of four experiments.

We next tested whether apoptosis induced by mCD95L was affected by FynC-GFP-INP54p expression. While DT40 cells expressing the CD95L(DA4) mutant induced apoptosis in FynC-GFP^{+} BJAB cells (Figure 2D, left panels), apoptosis was significantly attenuated at 16 and 24 h following engagement of CD95L(DA4) in FynC-GFP-INP54p^{+} BJAB cells (right panels). Concurrently, surface CD95 was downregulated in FynC-GFP^{+} BJAB cells at 30 and 60 min, but this was significantly compromised in FynC-GFP-INP54p^{+} BJAB cells (Figure 2E).

Expression of FynC-GFP-INP54p in BJAB cells inhibited CD95L-induced apoptosis irrespective of the degree of CD95 oligomerization. Expression of FynC-GFP-INP54p inhibited apoptosis and CD95 downregulation induced via soluble and plate-bound crosslinked Flag-CD95L or anti CD95 mAb (CH-11) (Supplementary Figure 5A). Finally, CD95 activation of
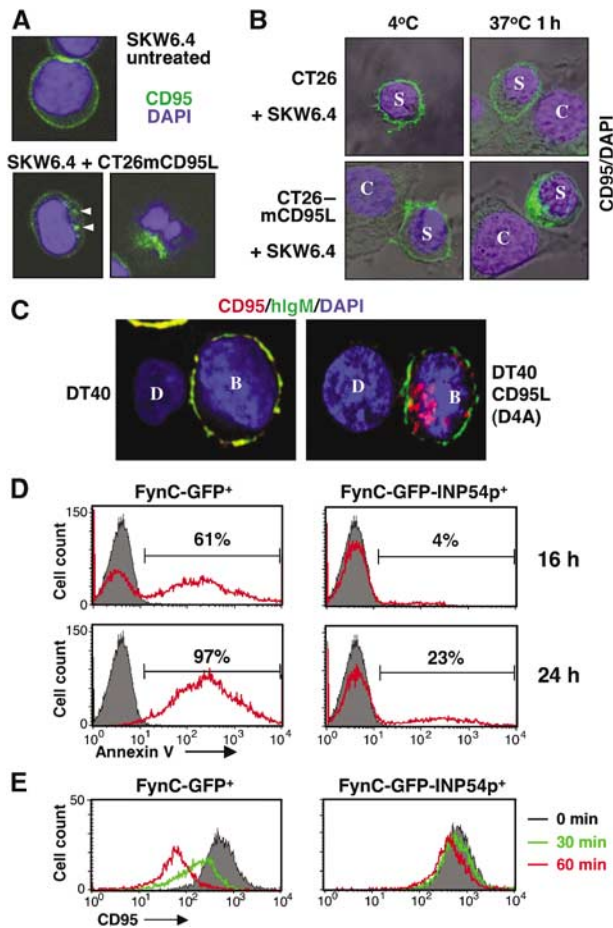
Figure 2 Membrane-bound CD95L induces internalization of CD95. (**A**) Internalization of CD95 on SKW6.4 cells following activation by mCD95L. SKW6.4 cells were incubated with FITC-DX2 on ice. Cells were then left untreated or incubated with detached CT26 cells expressing human mCD95L for 1 h. Nuclei were stained with DAPI and CD95 was visualized by confocal microscopy. The left bottom panel represents an early stage with intact nucleus and internalized CD95-containing vesicles (arrowheads). The right bottom panel shows a more advanced stage of apoptosis with nuclear fragmentation. (**B**) CD95 on SKW6.4 cells internalizes at the contact side with mCD95L-expressing CT26 cells. SKW6.4 cells (labeled S) with a bound biotin-labeled anti-CD95 mAb were plated on top of adherent CT26 or CT26mCD95L cells (labeled C) and incubated as indicated. CD95 was visualized by staining with streptavidin Alexa Flour 488. Nuclei were visualized by DAPI staining. (**C**) Internalization of CD95 on BJAB cells following activation by cleavage-resistant mCD95L(DA4). BJAB cells (labeled B) were incubated with chicken DT40 cells (labeled D) (left panel) or DT40 cells expressing human mCD95L(DA4) (right panel) for 1 h and then analyzed by deconvolution microscopy for CD95 (red), surface hIgM (green) and DAPI staining (blue). (**D**) Inhibition of mCD95L-induced apoptosis in FynC-GFP-INP54p-expressing cells. BJAB cells were transfected with FynC-GFP-INP54p or control FynC-GFP and incubated with DT40 cells expressing a noncleavable mutant of human mCD95L(DA4) at a ratio of 1:5 (BJAB:DT40) for the indicated times. Apoptosis of GFP⁺ cells was assessed by staining with Annexin V. Data shown are representative of two independent experiments. (**E**) Inhibition of mCD95L-mediated CD95 downregulation in FynC-GFP-INP54p-expressing cells. BJAB cells, transfected as described in D, were incubated with DT40 cells expressing mCD95L(DA4) for 30 or 60 min. Surface CD95 expression on GFP⁺ cells was assessed by flow cytometry. Data shown are representative of two independent experiments.

BJAB cells using beads covalently coupled with an anti-CD95 mAb or Flag-CD95L was also inhibited by expression of FynC-GFP-INP54p (Supplementary Figure 5B and data not shown). In contrast to the agonistic anti-CD95 mAbs, treatment of H9 cells with an antagonistic anti-CD95 mAb (ZB4) failed to induce CD95 internalization (Supplementary Figure 5C). Hence, independent of the methodology of stimulation, expression of FynC-GFP-INP54p inhibits CD95 internalization and apoptosis. Moreover, apoptosis is dependent on internalization of CD95 in cells treated with sCD95L or mCD95L.

Clathrin-mediated endocytosis is required for CD95-induced apoptosis

Our data suggested that modulation of PIP_2 levels through INP54p rendered cells resistant to CD95-mediated apoptosis by blocking internalization of CD95. However, modulation of PIP_2 could result in global cellular changes that could cause cells to become resistant to CD95-mediated apoptosis by mechanisms other than receptor internalization. CD95 has been suggested to internalize through a clathrin-mediated endocytic pathway (Algeciras-Schimnich *et al*, 2002). To specifically interfere with this form of receptor internalization, we targeted expression of the AP-2 adaptor complex and clathrin heavy chain (CHC) proteins using RNA interference. Transfection of siRNAs specific for CHC or AP-2($\alpha \pm \mu_2$) adaptor subunits resulted in significant reduction in their levels of protein expression (Figure 3A, lanes 2–6) (Motley *et al*, 2003).

Correspondingly, knockdown of AP-2 (α or μ_2) alone resulted in a moderate decrease in CD95L-induced down-regulation of surface CD95 (Figure 3B, panels 2 and 3). Knockdown of both AP-2 (α and μ_2) subunits or CHC resulted in a greater compromise in CD95 downregulation (panels 4 and 5). Finally, knockdown of both AP-2($\alpha + \mu_2$) and CHC resulted in the greatest inhibition of CD95 downregulation, though the basal level of surface CD95 expression was also decreased (panel 6).

The degree of compromise observed in CD95 downregulation directly correlated with the degree of apoptosis induced by CD95L. Gene knockdown of either AP-2($\alpha + \mu_2$) or CHC resulted in ~50–80% decrease in CD95L-induced apoptosis, respectively, and the combination of AP-2($\alpha + \mu_2$) and CHC siRNAs, which demonstrated the greatest inhibition in CD95L-induced CD95 downregulation, resulted in total protection from CD95L-induced apoptosis (Figure 3C).

Interestingly, the inducible association of FADD with CD95 was compromised in cells transfected with AP-2($\alpha + \mu_2$) or CHC siRNAs (Figure 3D, lanes 3 and 4). The lack of FADD association severely reduced the formation of the DISC as neither FADD nor caspase-8 co-immunoprecipitated with CD95 at 5, 15 or 30 min following CD95 activation in cells transfected with CHC siRNAs (Figure 3E). These results suggest a role of receptor internalization in assembly of the DISC.

Finally, we analyzed the role of CD95 internalization in CD95L-induced apoptosis with peripheral human T lymphocytes (PBTs). PBTs were activated through CD3/CD28 and then transfected with siRNAs for AP-2($\alpha + \mu_2$) and GFP, the latter of which was utilized to monitor expression. GFP^hi cells were purified by cell sorting and analyzed for CD95 internalization and apoptosis. Transfection of AP-2($\alpha + \mu_2$) siRNAs in PBTs resulted in inhibition of CD95 downregulation following CD95L activation (Figure 3F, left bottom
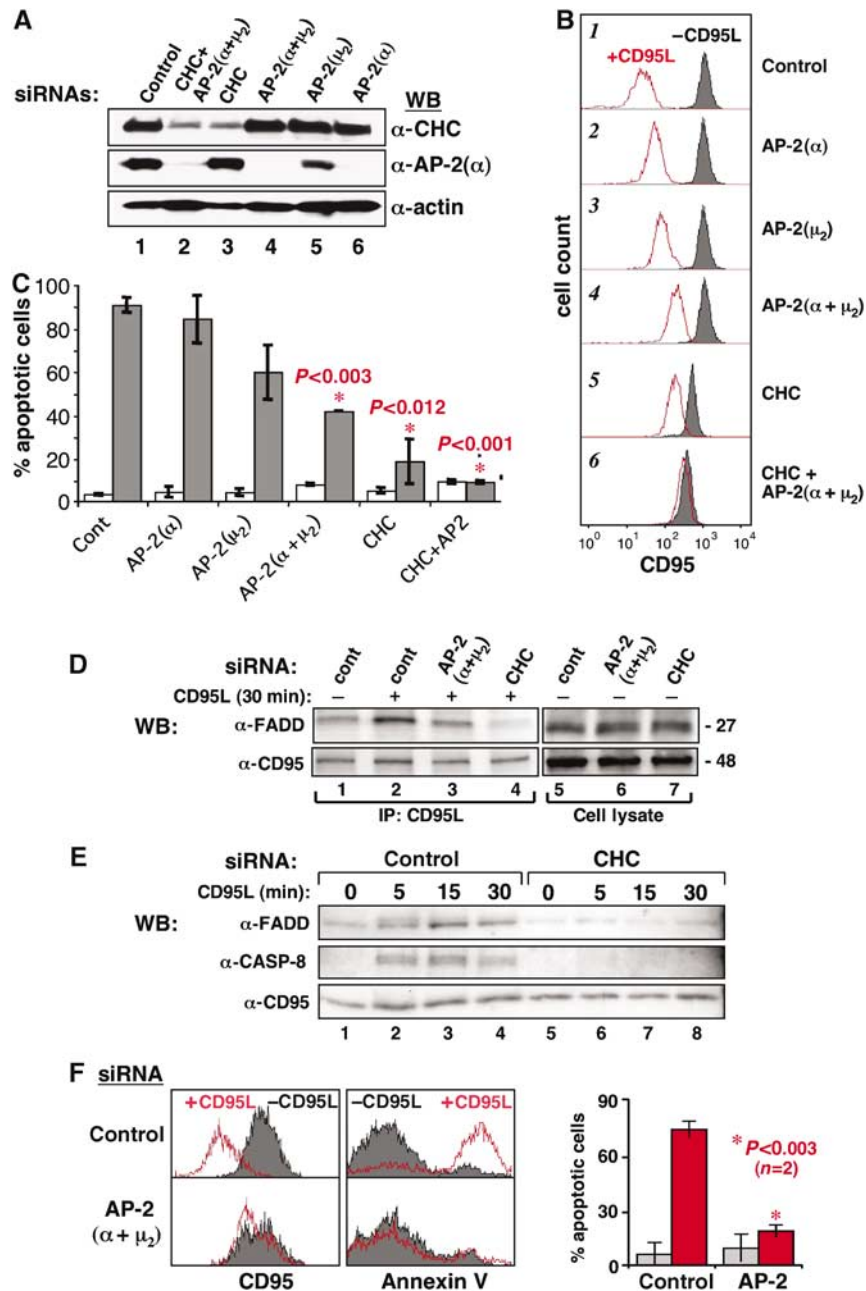
Figure 3 Clathrin-mediated endocytosis is required for CD95 downregulation and apoptosis. (**A**) Knockdown of CHC, AP-2 μ_2 and AP-2 α using siRNAs in BJAB cells. Efficiency of knockdown was monitored by blotting for the indicated proteins. Blotting for actin was used as a control for protein loading (bottom). (**B**) BJAB cells transfected with the indicated siRNAs, as described in (A), were incubated with Flag-CD95L for 30 min and surface CD95 expression assessed by flow cytometry. Red histograms indicate cells stimulated for 30 min, while the gray shadowed areas indicate basal levels of CD95 without CD95L stimulation. Data shown are representative of three experiments. (**C**) BJAB cells, as described in (A) and (B), were incubated in the presence (grey) or absence (white) of Flag-CD95L for 16 h and apoptotic cells quantified by staining with Annexin V and 7-AAD. Data shown are representative of three experiments. (**D**) CD95L-induced association of FADD with CD95 is inhibited by AP-2 and CHC siRNAs. Cells were transfected with control (lanes 1 and 2), AP-2 (lane 3) or CHC (lane 4) siRNAs, activated with Flag-CD95L for 30 min and FADD association with activated CD95 assessed by immunoprecipitating CD95L–CD95 complexes. Lanes 5–7 demonstrate comparable levels of FADD and CD95 in all cells. (**E**) FADD and caspase-8 association with CD95 is inhibited by CHC siRNAs. BJAB cells were transfected with control (lanes 1–4) and CHC (lanes 5–8) siRNAs and activated with Flag-CD95L for the indicated times. Association of FADD and caspase-8 with activated CD95 was assessed by immunoprecipitating for CD95L and immunoblotting for FADD, caspase-8 and CD95. (**F**) Clathrin-mediated endocytosis is required for CD95-mediated apoptosis in PBTs. Activated human CD4$^+$ PBTs were transfected with siRNAs for AP-2($\alpha + \mu_2$) and a GFP cDNA to monitor expression efficiency. Sorted GFP^{hi} cells were analyzed for CD95 downregulation (left) and apoptosis (right) following Flag-CD95L activation (30 min and 6 h, respectively). Red histograms indicate cells stimulated with CD95L while grey shadowed areas represent untreated cells. % apoptotic cells are quantified on the right. Data shown are representative of two experiments.

panel). Correspondingly, these cells demonstrated compromised CD95L-induced apoptosis (Figure 3F, right bottom panel). In summary, our data indicated that inhibition of

CD95 internalization in type I cells as well as in primary T lymphocytes attenuated recruitment of DISC components to CD95 receptors and apoptosis.

Recruitment of DISC components following CD95 internalization

To directly follow the recruitment of DISC components to activated CD95 and to compare receptor signaling between type I and type II cells, we made use of a novel method to isolate receptor-containing internalized vesicles that has been used to detect internalizing TNF receptor and its signaling components (Schneider-Brachert *et al*, 2004). In this method, cells were incubated with biotinylated anti-CD95 (anti-APO-1) mAb, followed by addition of streptavidin coupled magnetic nanoparticles. Following internalization, cells were homogenized and magnetic vesicles isolated in a free flow apparatus employing a high-gradient magnetic field. Western blotting of receptor-containing vesicles for endosomal and lysosomal markers was performed to assess the different endocytic maturation stages of receptor-containing vesicles.

Consistent with the ability of CD95 to internalize in type I SKW6.4 cells, Rab4 and EEA-1, markers for endosomal trafficking, were readily detected within CD95-containing vesicles very early after stimulation and peaking at 10 min (Figure 4A). Already detectable at 3 min and peaking at 30 min, CD95-containing vesicles also had lysosomal characteristics as evidenced by the appearance of cathepsin D (CatD), suggesting rapid association/fusion of CD95-containing receptosomes with CatD-containing lysosomal compartments. While a low level of FADD was detected in CD95 containing membrane structures at basal levels, its appearance in magnetic vesicles peaked at 30 min. Similar to FADD, caspase-8 and its intermediate cleavage products peaked at 10 min and could be detected as late as 3 h following stimulation (data not shown), and suggested that most of the caspase-8 activation occurred while inside the cells located on endosomal and even lysosomal vesicles. A similar kinetics for association of caspase-10 within the CD95-containing vesicles was also observed.

In contrast to type I SKW6.4 cells, no significant increase in Rab4, EEA-1 or CatD was observed in type II Jurkat cells, suggesting a lack of directional movement of CD95 into endosomal vesicles (Figure 4B). Consistent with the delayed and lower amounts of DISC component assembly in type II cells, FADD, caspase-8 and -10 were detected at lower levels and at later time points than in type I cells.

Since differences observed between type I SKW6.4 and II Jurkat cells might be due to the lower levels of CD95 expression on type II cells or limited to only lymphoid cells (Huang *et al*, 2000), we analyzed type I ACHN cells that express lower levels of CD95 than type II HCT15 cells (Algeciras-Schimnich *et al*, 2003). Rab4 was detected within CD95-containing vesicles with maximal association at 5 min in ACHN cells, indicating that receptor internalization had already begun (Figure 4C). EEA-1 appeared at 5 min and peaked at 30 min, consistent with maturation to endosomal vesicles. CatD was also detected at 5 min with further increases to 60 min indicative of movement of CD95 and its associated proteins into the lysosomal compartment. Analysis of DISC components revealed that recruitment of FADD, caspase-8 and -10 as well as caspase-8 activation peaked at 30 min, a time point at which most of the receptor had moved into an EEA-1-containing compartment. In contrast to type I ACHN cells, Rab4, EEA-1 and CatD demonstrated minimal increases following stimulation in type II HCT15 cells (Figure 4D). Moreover, FADD, caspase-8 and -10 were only weakly detected in CD95-

containing membranes at 60 min. Together, these data suggest that in type I cells, both of hematopoietic and nonhematopoietic origin, most of the DISC components were recruited to CD95 after its internalization into endosomal/lysosomal compartments.

Colocalization of CD95, FADD and active caspase-8 on endosomes following CD95 stimulation

To complement the biochemical studies, we analyzed the subcellular localization of FADD in untreated and CD95L-activated BJAB cells by deconvolution microscopy. For FADD, both nuclear as well as cytoplasmic staining have been described (Perez and White, 1998; Gomez-Angelats and Cidlowski, 2003; Screaton *et al*, 2003; O'Reilly *et al*, 2004). In untreated BJAB and PBTs, FADD was preferentially detected within the nucleus based on its colocalization with DAPI nuclear staining (Supplementary Figure 6A, panels 1 and 4 and data not shown). While there was minimal overlap of staining for EEA-1 with FADD in untreated cells (panel 3), overlap of FADD and EEA-1 was readily detected 5 min following CD95L activation (panel 7). Subcellular fractionation studies confirmed a predominant nuclear localization of FADD in untreated BJAB cells and the nuclear and cytoplasmic distribution in CD95L-treated BJAB cells (Supplementary Figure 6B). In contrast, confocal and fractionation studies demonstrated no change in the nuclear and cytoplasmic distribution of FADD in untreated and CD95-stimulated Jurkat T cells (Supplementary Figures 6C and D).

Analysis of CD95 and FADD localization in untreated and CD95-stimulated BJAB cells further supported their colocalization on early endosomes following CD95L engagement. In untreated BJAB cells, CD95 was expressed at the PM and not co-localized with FADD (Figure 5A, panels 1–3). Within 2 min following CD95L stimulation, CD95 had formed microaggregates at the PM and FADD was readily detected in the cytoplasm (panels 6–8). At 15 min following CD95L engagement, when FADD association with CD95 was maximal in these cells (see Figure 1B), significant colocalization of CD95 and FADD was detected in a TfR$^+$ early endosomal compartment (Figure 5A, panels 11–15). Similarly, colocalization of CD95 and activated caspase-8 was readily detected within an EEA-1$^+$ compartment within 15 min following CD95L engagement (Figure 5B, panels 4–6, and Figure 5C) consistent with the analysis of CD95-containing receptosomes (see Figure 4).

The recruitment of DISC components to activated CD95 after internalization appears to be in contradiction to our previous report on a very rapid recruitment of FADD and caspase-8 to activated CD95 (Kischkel *et al*, 1995). However, these studies involved detergent lysis of cellular membranes causing destruction of intracellular compartments and did not permit discrimination of recruitment of DISC components to different cellular membranes. Hence, we utilized a biochemical approach that preserved intracellular membrane compartments by analyzing the subcellular localization of CD95 and its associated proteins after separating PM and endosomal membrane fractions. Using BJAB cells, CD95L activation resulted in a time-dependent decrease in the amount of CD95 within the PM fraction that was associated with a concomitant increase of CD95 detected within the endosomal fraction (Figure 5D). While a low level of FADD was co-immunoprecipitated with ligand-bound CD95 in untreated BJAB cells, no significant increase in FADD or
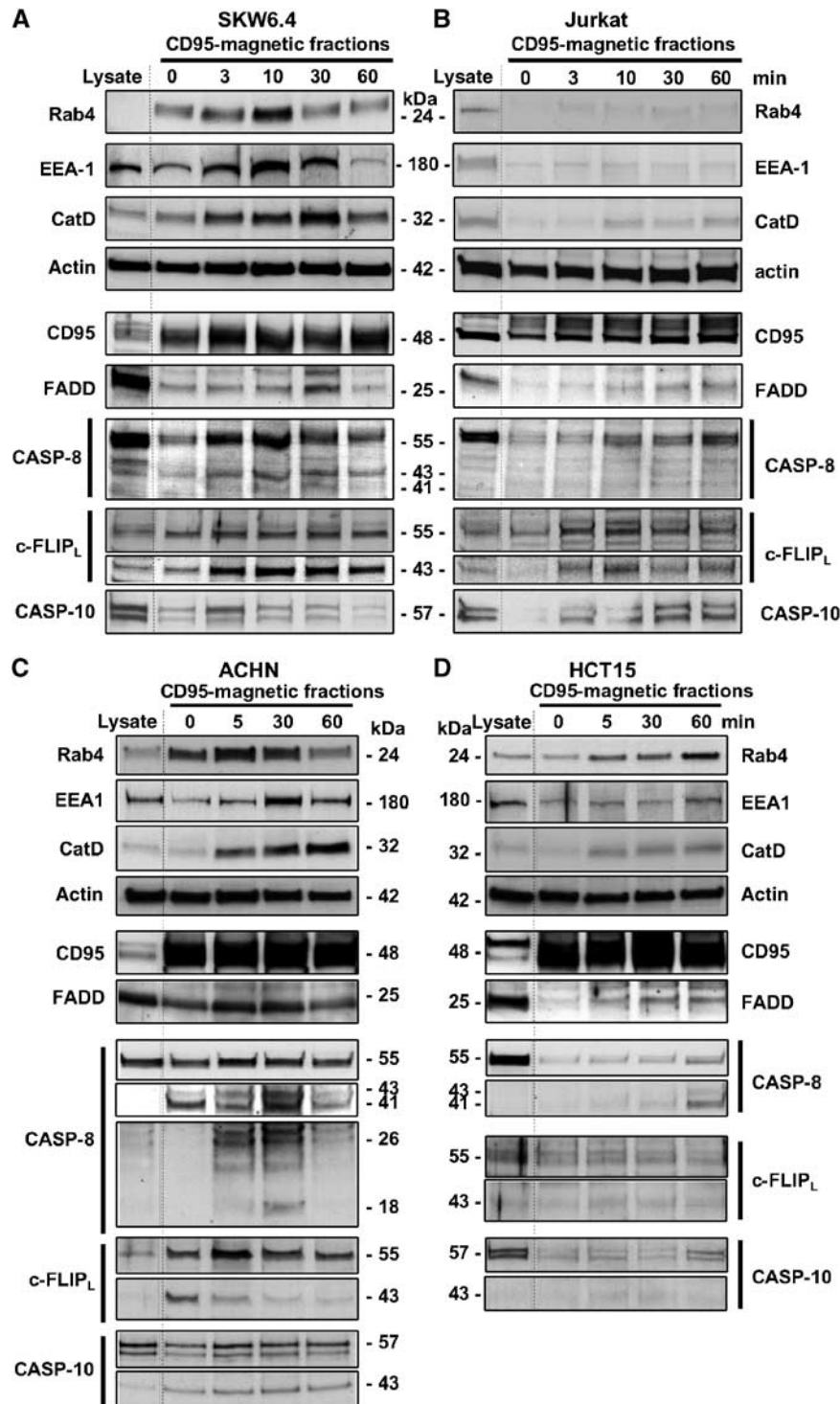
Figure 4 Internalization and endosomal maturation of CD95 DISC complexes. Time course of intracellular CD95-receptosome trafficking in SKW6.4 (**A**) and Jurkat (**B**) cells. Total cell lysates or magnetic fractions derived after 0, 3, 10, 30 and 60 min of anti-APO-1 mAb treatment were analyzed for signature proteins of endosomal maturation (Rab4 and EEA-1), lysosomes (CatD), actin, CD95 and DISC proteins. Note: twice as much lysate proteins were loaded to visualize Rab4, EEA-1 and CatD in the Jurkat cells. Time course of intracellular CD95-receptosome trafficking in ACHN (**C**) and HCT15 (**D**) cells. Total cell lysates or magnetic fractions derived after anti-APO-1 mAb treatment were analyzed as described in A and B.

activated caspase-8 was co-immunoprecipitated with PM-associated CD95 following CD95L engagement. In contrast, increased amounts of FADD and caspase-8 were co-immuno-precipitated with activated CD95 within the endosomal membrane fraction (lanes 5–7), with kinetics consistent with observed internalization of CD95 in these cells.

Mutation of a putative AP-2-binding motif disrupts CD95 internalization and apoptosis

The cytoplasmic domain of CD95 contains a putative protein-sorting motif (Y^{291}DTL), consistent with the consensus YXXΦ AP-2-binding sequence (Ohno et al, 1995). Similar to the reduction in CD95 internalization in the AP-2 knockdown

studies (Figure 3), internalization of a mutant CD95, in which Tyr 291 was changed to phenylalanine, following anti-CD95 mAb (CH-11) treatment, was diminished as compared to wt CD95 (Figure 6A). Concomitantly, the ability of CD95(Y291F) expressing cells to undergo apoptosis following treatment with an anti-CD95 mAb (CH-11) was similarly reduced (Figure 6B, lower two panels, and Figure 6C). As this tyrosine residue was localized within the FADD DD, we analyzed the *in vitro* ability of the DD of FADD to interact with the intracellular domains (ICDs) of wt CD95 or CD95(Y291F). ICDs

derived from either wt or Y291F were similarly capable of binding *in vitro* translated FADD (Figure 6D). In contrast, the DD incorporating the mutation found in *lpr^{cg}* mice did not bind FADD (Martin *et al*, 1999). Hence, mutation of Tyr 291 within the consensus AP-2-binding motif of CD95 compromised CD95L-mediated internalization and apoptosis, but not its ability to potentially interact with FADD. Together, our studies utilizing biochemical, genetic and imaging approaches indicate that CD95 internalization is required for efficient DISC assembly and activation of proapoptotic pathways.
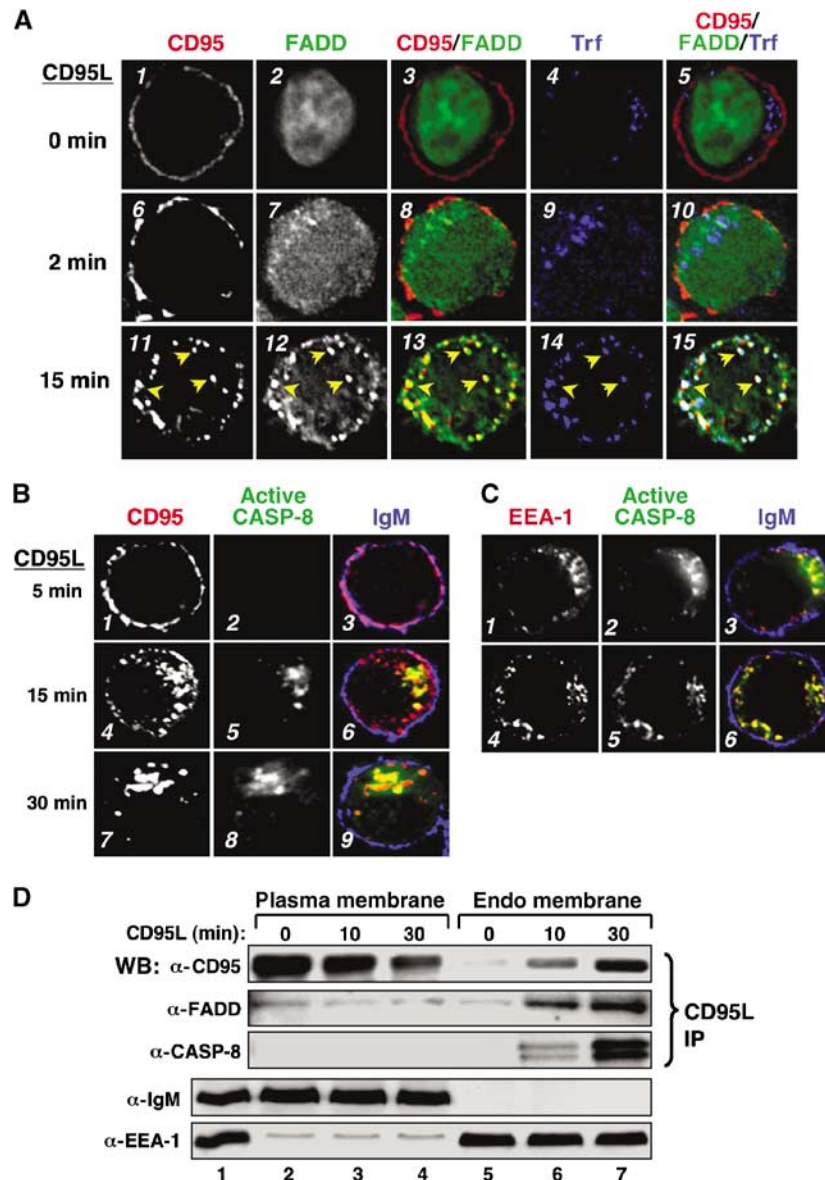

Figure 5 Colocalization of CD95, FADD and activated caspase-8 on early endosomes following CD95L stimulation. (**A**) BJAB cells were preincubated with Cy5-labeled transferrin (blue) for 15 min, left unstimulated or stimulated with Flag-CD95L for 2 or 15 min, then fixed and stained for CD95 (red) or FADD (green). Individual and overlay fluorescence are shown in deconvolution analysis. Data shown are representative of >200 cells analyzed. (**B**) Activated caspase-8 colocalizes with internalized CD95. BJAB cells were stimulated with Flag-CD95L. Cells were fixed and stained for CD95 (left), cleaved (active) caspase-8 (middle) or IgM. Merged images stained for CD95 (red), active caspase-8 (green) and IgM (blue) as a PM marker are shown on the right (panels 3, 6 and 9). Data shown are representative of >100 cells analyzed. (**C**) Activated caspase-8 co-localizes with EEA-1 ⁺ endosomes. BJAB cells, treated with Flag-CD95L for 15 min, were fixed and stained for EEA-1 (left), activated caspase-8 (middle) or IgM. Merged images stained for EEA-1 (red), activated caspase-8 (green) and IgM (blue) are shown on the right (3 and 6). (**D**) BJAB cells were stimulated with Flag-tagged CD95L. PM (lanes 2–4) and endo membrane (lanes 5–7) fractions were separated from total cellular membrane extract (lane 1). Following fractionation, association of FADD and caspase-8 with activated CD95–CD95L complexes was analyzed by immunoblotting for FADD and caspase-8. Plasma and endo-membrane fractions were also immunoblotted for IgM as PM and EEA-1 as endosomal markers.
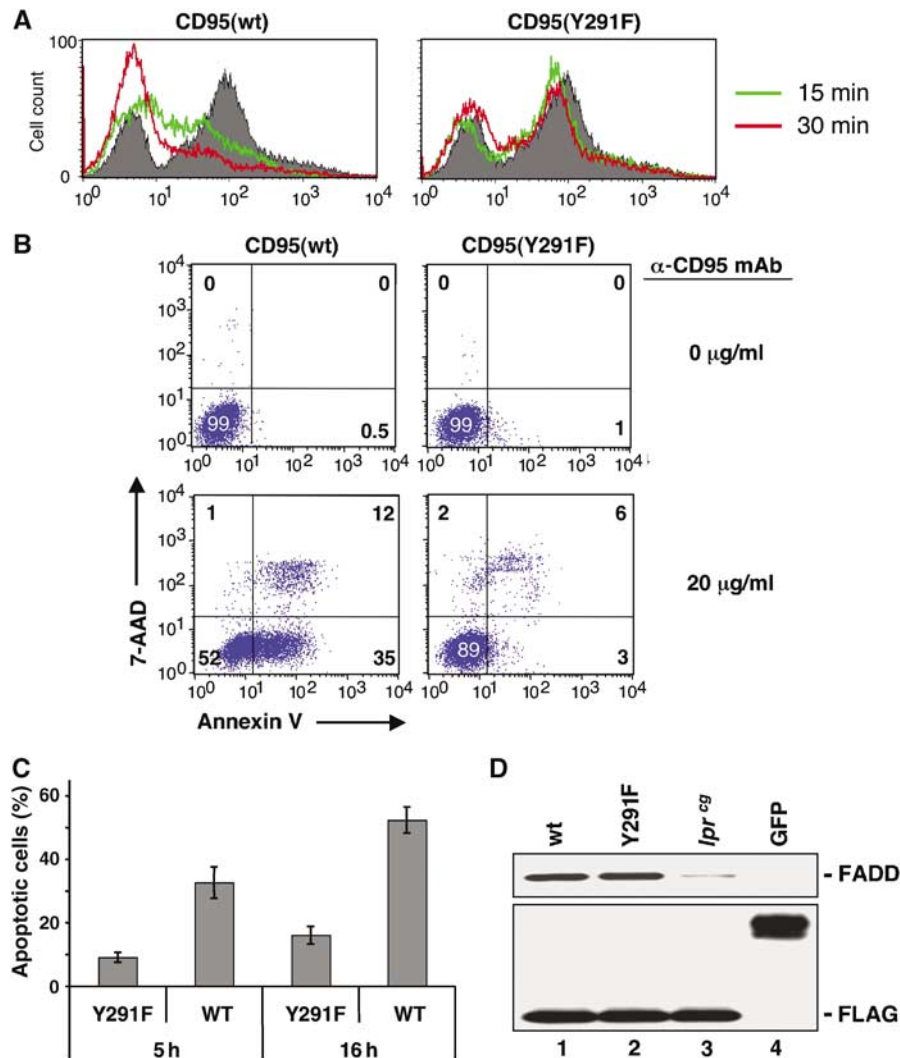
Figure 6 Internalization mutant of CD95(Y291F) is compromised in CD95L-mediated apoptosis. (**A**) A20 cells were transfected with wt human (h)CD95 or hCD95(Y291F). Cells were analyzed for CD95 downregulation following anti-hCD95 (CH11) activation at 0 (gray shadowed area), 15 (green) and 30 (red) min. (**B**) A20 cells were transfected with wt hCD95 or hCD95(Y291F). Cells were analyzed for apoptosis using the AnnexinV/7-AAD assay following anti-hCD95 (CH11) activation for 16 h. Data shown are representative of three experiments. (**C**) A20 cells were transfected with wt hCD95 or hCD95(Y291F). % apoptotic cells were quantified following incubation with an anti-hCD95 (CH11) mAb for 5 and 16 h. (**D**) CD95(Y291F) can bind FADD *in vitro*. The *in vitro* translated ICDs of wt CD95 (lane 1), internalization mutant CD95(Y291F) (lane 2), or the corresponding hCD95 mutation(V254N) in *lpr^{cg}* mice (lane 3) fused to a FLAG epitope was incubated with a biotinylated FADD DD. Flag-CD95-bound FADD was immunoprecipitated using anti-Flag mAb-coupled beads and analyzed by blotting for FADD and Flag. Flag-epitope-tagged GFP was used as a control protein (lane 4).

CD95-mediated signaling independent of CD95 internalization

CD95 engagement in CD95-resistant tumor cells or in CD95 apoptosis-sensitive type I tumor cells treated with sCD95L has been demonstrated to activate nonapoptotic signaling pathways, including Erk and NF-κB (Ahn *et al*, 2001; Qin *et al*, 2002; Barnhart *et al*, 2004). While our data indicated that receptor internalization in type I cells was required for activation of proapoptotic pathways, we examined the requirement of receptor internalization for CD95L-induced nonapoptotic signaling pathways: Erk1/2 phosphorylation and NF-κB transcriptional activation. Cells transfected with control siRNAs and treated with Flag-CD95L demonstrated no significant Erk1/2 activation (Figure 7A, lanes 1–3). By contrast, cells transfected with AP-2(α+μ₂) or CHC siRNAs showed CD95L-induced Erk1/2 activation (lanes 5–7 and 9–11). BJAB cells transfected with FynC-GFP-INP54p also

induced a dose-dependent increase in NF-κB responsive luciferase reporter, while cells transfected with FynC-GFP control had no NF-κB response as all cells had undergone apoptosis following CD95L stimulation (Figure 7B and data not shown). In both experimental systems, Erk and NF-κB responses remained intact when cells were stimulated through the B-cell antigen receptor or with phorbol 12-myristate 13-acetate (PMA). Crosslinking of the internalization defective CD95(Y291F) mutant also induced Erk activation, even more efficiently than the wt receptor (Figure 7C).

Isotype switch variants of the anti-APO-1 mAb have been reported to exhibit markedly distinct cellular activities (Dhein *et al*, 1992; Oehm *et al*, 1992). While the widely used IgG3 anti-APO-1 mAb induced apoptosis of type I SKW6.4 and H9 cells, the IgG2b switch variant of anti-APO-1, with identical specificity and affinity for CD95, does not induce apoptosis (Dhein *et al*, 1992; Supplementary Figure 7A). Consistent
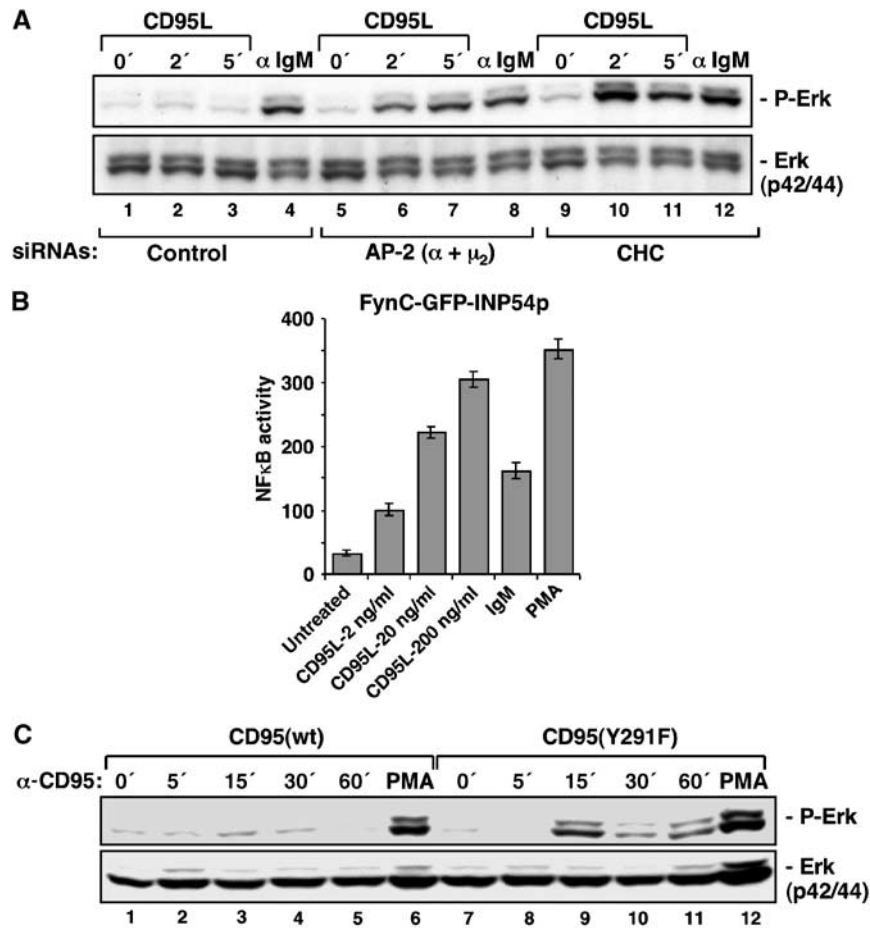
Figure 7 CD95L-mediated internalization-independent signaling. (**A**) Activation of Erk signaling pathway in cells transfected with AP-2($\alpha + \mu_2$) or CHC siRNAs. BJAB cells, transfected with control, AP-2($\alpha + \mu_2$) or CHC siRNAs, were incubated with Flag-CD95L for the specified times or anti-IgM Fab$_2'$ for 5 min. Cell lysates were analyzed for phospho-Erk1/2 (top) or total Erk1/2 (bottom) expression. Data shown are representative of two experiments. (**B**) Activation of NF-κB transcription in FynC-GFP-INP54p$^+$ cells. BJAB cells transfected with FynC-GFP-INP54p were analyzed for transcriptional activation of NF-κB following Flag-CD95L, PMA or BCR stimulation. These data are representative of two experiments. (**C**) Activation of Erk signaling pathways by CD95(Y291F). A20 cells, transfected with wt CD95 or CD95(Y291F), were incubated with anti-hCD95 mAb (CH11) for the specified times. Cell lysates were analyzed for phospho-Erk1/2 (top) or total Erk1/2 (bottom) expression. Cells were also treated with PMA as a positive control.

with the ability of the IgG3 backbone to self-aggregate through Fc–Fc interactions to induce cytotoxicity, additional crosslinking of the IgG2b anti-APO-1 mAb with protein A resulted in cellular apoptosis (Supplementary Figure 7A). While the IgG3 anti-APO-1 mAb rapidly induced capping, clustering and internalization of CD95, the nonapoptotic IgG2b anti-APO-1 mAb was unable to induce capping or internalization of CD95 (Figures 8A and B), though the IgG2b anti-APO-1 was able to stain CD95 as small surface structures consistent with the described signaling protein oligomerization structures (SPOTS) (Muppidi and Siegel, 2004; Siegel et al, 2004). Moreover, the IgG3, but not the IgG2b, anti-APO-1 mAb induced DISC formation in type I SKW6.4 and H9 cells (Figure 8C, lanes 1–8). Hence, the ability of the anti-APO-1 mAb to induce DISC assembly and apoptosis was associated with the ability of the anti-APO-1 mAb to induce CD95 internalization.

We further analyzed whether CD95 could activate non-apoptotic pathways when stimulated by the IgG2b and IgG3 anti-APO-1 mAbs. MCF7(FV) and MCF7(FB) cells, which have been extensively characterized with respect to induction of nonapoptotic pathways through CD95 and the resulting functional consequences, were chosen for this analysis (Stegh

et al, 2002). Isolation of magnetic internalizing vesicles demonstrated that MCF7(FV) cells activated by the IgG3 anti-APO-1 mAb maximally recruited DISC components, co-incident with the presence of endosomal EEA-1 and Rab4 markers (Supplementary Figure 7B). Similarly, maximal processing of caspase-8 was detected 60 min after CD95 stimulation, again consistent with the requirement of receptor endocytosis for activation of proapoptotic signaling pathways. Consistent with the differential abilities of the two isotype anti-APO-1 mAbs to induce apoptosis in MCF7(FV) cells, the proapoptotic IgG3 anti-APO-1 mAb efficiently induced DISC assembly, while DISC assembly was not detected with the nonapoptotic IgG2b anti-APO-1 mAb (Figure 8C, lanes 9–12). However, treatment of MCF7(FV) with the noninternalizing IgG2b anti-APO-1 mAb induced both NF-κB and Erk activation (Figures 8D and E). Similar data were observed for ACHN and MCF7(FB) cells treated with the IgG2b anti-APO-1 mAb (data not shown). Finally, we tested the ability of both CD95L and non-apoptotic anti-APO-1 to modulate cellular motility and invasiveness. Both CD95 stimuli enhanced in vitro cellular motility and invasiveness using MCF7(FB) cells (Figure 8F). Hence, signaling through noninternalization-inducing stimuli can activate a multitude
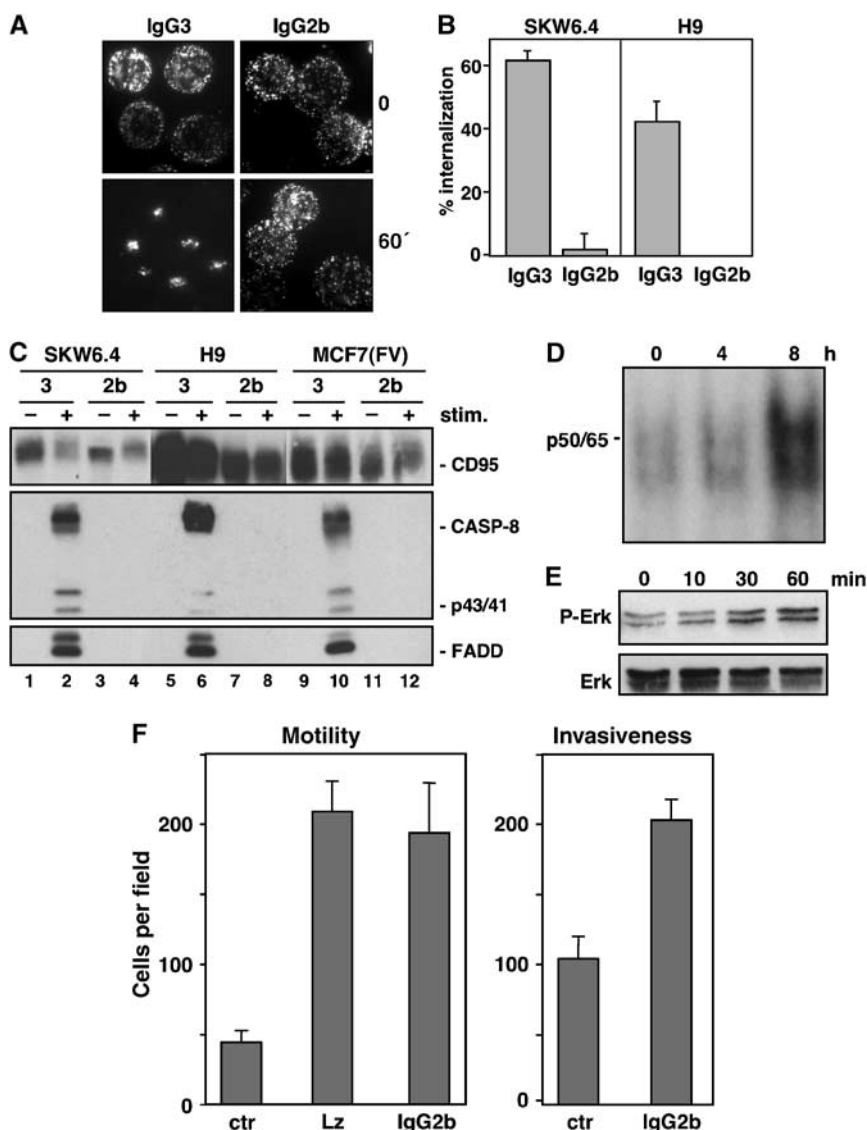
Figure 8 Activation of nonapoptotic signaling by anti-APO-1 IgG2b that does not induce CD95 internalization or apoptosis. (**A**) Effects of FITC-conjugated IgG3 (left two panels) and IgG2b (right two panels) anti-APO-1 mAbs on CD95 clustering in SKW6.4 cells was analyzed by fluorescence microscopy after 1 h of stimulation. (**B**) SKW6.4 cells were treated with either IgG3 or IgG2b anti-APO-1 mAbs for 1 h at 37°C. The number of cells with internalized CD95 following 1 h of Ab treatment was quantified. The experiment was performed in triplicates and is shown as the $\mu \pm$ s.d. (**C**) SKW6.4, H9 or MCF7(FV) cells were treated with IgG3 (lanes 1, 2, 5, 6, 9 and 10) or IgG2b (lanes 3, 4, 7, 8, 11 and 12) anti-APO-1 mAbs. Activated CD95 molecules were immunoprecipitated and analyzed by Western blotting for CD95 (C20), caspase-8 and FADD. (**D**) EMSA analysis of MCF7(FV) cells using a ^{32}P-labeled oligonucleotide carrying NF-κB-binding sites stimulated with 1 μg/ml IgG2b anti-APO-1 for the indicated times. p50/p65 denotes the migration of the NF-κB heterodimer. (**E**) MCF7(FV) cells stimulated with 1 μg/ml IgG2b anti-APO-1 for the indicated times were analyzed for pErk and total Erk by Western blotting. (**F**) MCF7(FB) cells, treated with control (ctr), LzCD95L or IgG2b anti-APO-1 mAb, were analyzed using *in vitro* motility (left) or invasiveness (right) assays.

of signaling pathways that can contribute to enhanced tumorigenic potential, whereas internalization of CD95 is only required for apoptosis signaling.

Discussion

Receptor internalization is required for CD95L-induced apoptosis in type I cells

Formation of the DISC represents a critical step in the initiation of apoptosis induction through CD95 (Cremesti *et al*, 2001; Grassme *et al*, 2001; Algeciras-Schimnich *et al*, 2002). In this report, we utilized six distinct experimental approaches to demonstrate an unexpected role for receptor endocytosis in DISC assembly and apoptosis in CD95 signal

transduction in type I cells. The first strategy involved selective modulation of PIP$_2$ levels that impaired internalization of CD95. The second strategy utilized siRNAs that target the clathrin endocytic machinery. The third involved the concordance of different switch isotypes of an anti-APO-1 mAb to induce CD95 internalization, DISC formation and apoptosis. The fourth involved a selective internalization mutant in the cytoplasmic domain of CD95. The fifth utilized a novel technique to directly follow internalizing receptosomes containing CD95 and the sixth involved subcellular fractionation studies—all of which demonstrate that DISC assembly occurs predominantly after CD95 has internalized and has entered an early endosomal compartment. Additionally, confocal microscopy of activated cells indicates that

CD95 co-localizes with FADD and activated caspase-8 on an EEA-1$^+$ compartment. While the initiation of DISC assembly may occur prior to and/or independent of receptor internalization, these data support an important role of CD95 internalization for efficient assembly of DISC components, activation of caspase-8 and -3, and induction of cellular apoptosis in type I, but not type II, cells. Hence, CD95 internalization in type I cells plays a requisite positive function rather than an inactivating function that would otherwise be biologically counterproductive for a cell destined for apoptosis.

A recent study has demonstrated that the assembly of activated TNF-R1 complexes with FADD, TRADD and caspase-8 was also dependent on receptor endocytosis (Schneider-Brachert *et al*, 2004). An internalization-deficient TNF receptor, while capable of recruiting RIP1 and TRAF2 at the PM, was unable to initiate DISC formation and induce apoptosis (Schneider-Brachert *et al*, 2004). Our study now provides the first evidence for a member of the subgroup of death receptors that directly recruit FADD (which includes CD95, DR4 and DR5), that the spatial and temporal regulation of membrane dynamics and internalization of receptors serves a critical regulatory function in defining cellular fate.

Receptor internalization and membrane-bound CD95L

Our studies also demonstrate a requirement for CD95 internalization in mCD95L-induced apoptosis. The ability of wt mCD95 and the mCD95L(DA4) mutant as well as covalently bound anti-CD95 mAb to induce internalization of CD95 and to activate apoptosis in BJAB and SKW6.4 cells supports the idea that CD95 must undergo some biophysical alteration induced by binding of ligand or agonistic mAbs. Receptor ligation results in the rapid formation of higher-ordered aggregates of CD95 within seconds following receptor cross-linking (Kischkel *et al*, 1995). High resolution confocal microscopy and live-cell imaging have recently revealed the formation of higher-ordered CD95 oligomers, termed SPOTS, at the PM following receptor engagement, a process that is dependent upon FADD association, but independent of caspase activation (Siegel *et al*, 2004). In addition, biochemical studies have demonstrated that CD95 is further recruited to raft membrane fractions, a process that is independent of its DD and DISC formation, following receptor activation (Eramo *et al*, 2004) (Figure 9). Hence, CD95L engagement induces spatial and conformational alterations in CD95 that permit receptor oligomerization, SPOT formation and localization within lipid rafts. Our studies define an additional requirement for the oligomerized CD95 to induce apoptosis: internalization through a clathrin-mediated pathway and delivery to the early endosomal compartment for efficient DISC assembly and amplification (Figure 9).

Potential role of the endosome in CD95 association with FADD

Internalized CD95 within the endosome also appears to provide a localizing signal to concentrate FADD. In the absence of CD95 internalization, FADD remained in a diffuse cytoplasmic pattern and demonstrated substantially decreased localization within the EEA-1$^+$ early endosomal
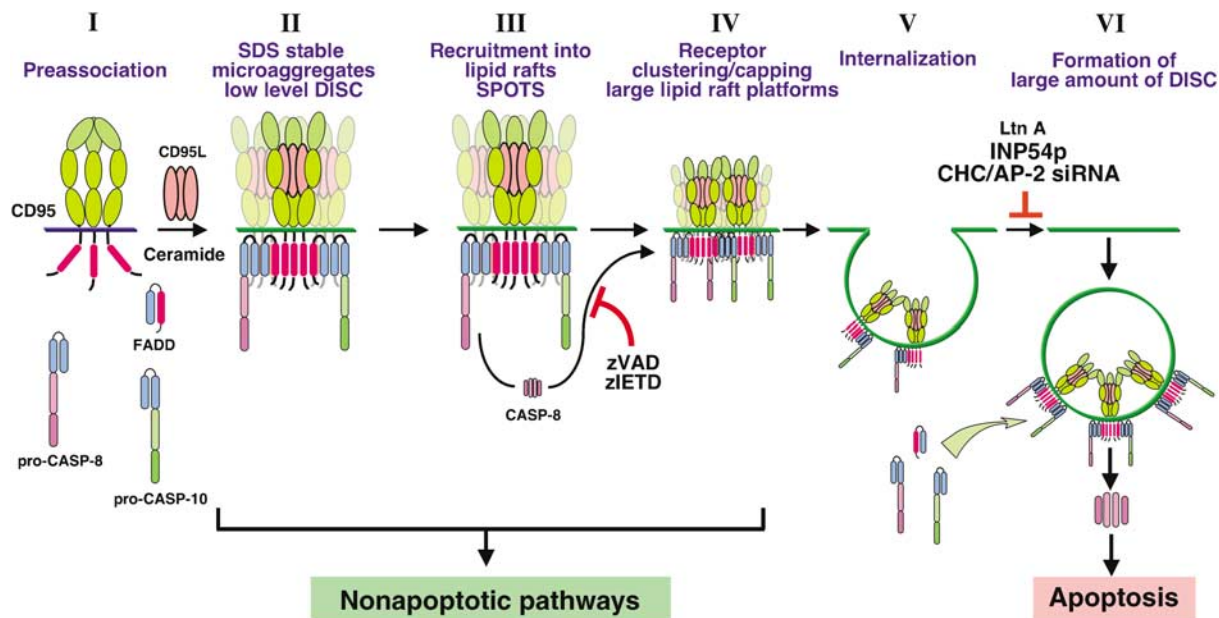

Figure 9 Model for early CD95 signaling. I, Ligand-independent receptor preassociation. II, Formation of microaggregates that are detected as SDS stable aggregates and low level of DISC formation. It was shown that cells expressing sphingomyelin synthase 1 form SDS stable aggregates more efficiently than SMS-negative cells (Miyaji *et al*, 2005), suggesting that ceramide, although not essential for CD95 signaling, is a general enhancer of CD95-mediated apoptosis. III, Recruitment of CD95 into lipid rafts to form SPOTS. IV, Receptor clustering also referred to as capping and formation of large lipid raft platforms. This step depends on generation of active caspase-8 by the DISC and can be efficiently prevented by preincubating cells with either zVAD-fmk or zIETD-fmk. In the absence of internalization, signals from steps 2–4 have the potential to activate nonapoptotic pathways, but are insufficient to kill type I cells. V, Internalization of the activated receptor. VI, Migration of internalized CD95 into an endosomal compartment and further recruitment of DISC components. This step is dependent on actin filaments since it can be inhibited by latrunculin A (LtnA). This step also requires PIP$_2$ and it is clathrin mediated, since it is inhibited by either overexpression of INP54p or downregulation of CHC or AP-2. In case of mCD95L-induced apoptosis, we postulate a ligand-induced internalization of an activated CD95 complex that no longer contains the ligand. DISC components are FADD/Mort1, caspase-8, caspase-10 and c-FLIP (not shown). Blue domains, DED; red domain, DD; the N-terminal PLAD in CD95 is shown in a different green tone.

compartment (data not shown). Hence, DISC assembly or amplification on endosomes may provide additional temporal and spatial regulation to transport the activated DISC to downstream effectors. The requirement for activation of caspase-8 inside cells is consistent with a previous study that found that active caspase-8 generated at and tethered to the PM does not kill cells (Martin *et al*, 1998).

Recent evidence for a variety of receptors supports a role for the endosome in the control of signal transduction. In the case of the EGF receptor, Grb2 and activated Ras colocalize not only at the PM, but also on endosomes following EGF stimulation (Di Guglielmo *et al*, 1994). In addition, p14 and MP1 members of the protein superfamily of small subcellular adaptor proteins (ProfIAP) are preferentially localized within the late endosome and complex with MEK1/2 to facilitate Erk1/2 activation (Wunderlich *et al*, 2001; Teis *et al*, 2002). Finally, the APPL (Adaptor protein containing PH domain, PTB domain and Leucine zipper motif) Rab5 effector proteins, localized within a subpopulation of endosomes, link EGF and oxidative stress signals with chromatin remodeling and gene transcriptional regulation (Miaczynska *et al*, 2004a). In addition to EGFR, targeting of the TNF-R1-associated DISC complex to *trans*-Golgi vesicles has been recently demonstrated to activate the endolysosomal acidic, but not the PM localized neutral, sphingomyelinase (Schneider-Brachert *et al*, 2004). Hence, the endosome localized signaling complex appears to provide a subcellular nidus for signal amplification and routing to appropriate downstream effectors.

Compartmentalization of CD95 signaling is important in defining cellular outcome

Our studies also indicate that alterations in the ability of CD95 to internalize have profound effects in the cellular fate of CD95-activated cells. Cells unable to internalize CD95, through expression of FynC-GFP-INP54p, downmodulation of the clathrin-AP-2/CHC endocytic machinery or through the use of nonapoptotic anti-CD95 mAbs, induce transcriptional activation of NF-κB and activation of Erk1/2 following CD95 engagement. Hence, additional types of signaling likely occur independent of receptor internalization. Activation of nonapoptotic signaling pathways, including MAPK and NF-κB signaling pathways, by CD95L has been suggested to play a role in the tumorigenesis of CD95-resistant tumors (Ahn *et al*, 2001; Barnhart *et al*, 2004; Peter *et al*, 2005). Indeed, treatment of CD95L-resistant MCF7(FB) cells with anti-APO-1 mAb or soluble CD95L increased tumor cell motility and invasiveness. Hence, the dynamics of CD95 membrane localization and internalization plays a critical role to balance internalization-dependent apoptotic and internalization-independent nonapoptotic pathways to drive cellular apoptosis and other functions, respectively.

The membrane dynamics of TNF-R1 have also been demonstrated to play a critical role in defining the cellular fate of TNFR activation. TNF-R1-induced apoptosis involves sequential signaling complexes. The first involves the assembly of a lipid raft-localized complex involving TNF-R1, TRADD, RIP1 and TRAF2 (complex 1) and mediates NF-κB activation prior to ubiquitinylation and degradation of the TNF-R1 complex (Legler *et al*, 2003; Micheau and Tschopp, 2003). Complex 1 undergoes yet-to-be defined modifications such that the DD of TRADD and RIP1, previously bound to TNF-R1, become available to interact with other DD-containing proteins. The recruitment of FADD and caspase-8 to this modified cytoplasmic complex initiates the cellular apoptotic machinery (complex 2) (Micheau and Tschopp, 2003). Complex 2 forms inside cells and does not contain the receptor. Recent studies tracking receptor-containing internalized vesicles, however, demonstrate that the DISC remains bound to the internalized TNF-R1 to form endosomal 'death-signaling vesicles' (Schneider-Brachert *et al*, 2004). For CD95, stimulation by CD95L induces formation of low level of DISC at the cell surface followed by internalization of the entire complex (Figure 9). In type I cells, this internalization step triggers recruitment of large amounts of the signaling proteins FADD and caspase-8 to the activated receptor on endosomes executing apoptosis.

Together, our results provide support for the view that the subcellular location of receptor signaling plays important roles in defining cellular fates. In the case of CD95, receptor internalization commits the cell to a proapoptotic outcome by delivering the activated receptor through an endosomal signaling pathway. Conversely, inhibition of receptor internalization enables the activated receptor to engage biochemical pathways that induce prosurvival pathways. These dynamics are not only critical in understanding CD95 biology but also may have important implications in understanding the effects of chemotherapeutic agents that affect receptor trafficking in combination with emerging proapoptotic treatments in cancer therapy.

Materials and methods

Antibodies used in this study are summarized in Supplementary Table I. Additional reagents are summarized in Supplementary Table II. Methods for cells, molecular construction of cDNAs, protein expression, immunofluorescence and receptor capping are described in Supplementary Figure 8. Methodologies for CD95 activation, DISC analysis, membrane fractionation, apoptotic and *in vitro* invasiveness assays, siRNA preparation and transfections are described in Supplementary Figure 9.

Supplementary data
Supplementary data are available at *The EMBO Journal* Online.

Acknowledgements

References

Ahn JH, Park SM, Cho HS, Lee MS, Yoon JB, Vilcek J, Lee TH (2001) Non-apoptotic signaling pathways activated by soluble Fas ligand in serum-starved human fibroblasts. Mitogen-activated protein kinases and NF-kappaB-dependent gene expression. *J Biol Chem* **276**: 47100–47106

Algeciras-Schimnich A, Peter ME (2003) Actin dependent CD95 internalization is specific for Type I cells. *FEBS Lett* **546**: 185–188

Algeciras-Schimnich A, Pietras EM, Barnhart BC, Legembre P, Vijayan S, Holbeck SL, Peter ME (2003) Two CD95 tumor classes

with different sensitivities to antitumor drugs. *Proc Natl Acad Sci USA* **100:** 11445–11450

Algeciras-Schimnich A, Shen L, Barnhart BC, Murmann AE, Burkhardt JK, Peter ME (2002) Molecular ordering of the initial signaling events of CD95. *Mol Cell Biol* **22:** 207–220

Barnhart BC, Alappat EC, Peter ME (2003) The CD95 type I/type II model. *Semin Immunol* **15:** 185–193

Barnhart BC, Legembre P, Pietras E, Bubici C, Franzoso G, Peter ME (2004) CD95 ligand induces motility and invasiveness of apoptosis-resistant tumor cells. *EMBO J* **23:** 3175–3185

Boldin MP, Varfolomeev EE, Pancer Z, Mett IL, Camonis JH, Wallach D (1995) A novel protein that interacts with the death domain of Fas/APO1 contains a sequence motif related to the death domain. *J Biol Chem* **270:** 7795–7798

Ceresa BP, Schmid SL (2000) Regulation of signal transduction by endocytosis. *Curr Opin Cell Biol* **12:** 204–210

Chinnaiyan AM, O'Rourke K, Tewari M, Dixit VM (1995) FADD, a novel death domain-containing protein, interacts with the death domain of Fas and initiates apoptosis. *Cell* **81:** 505–512

Cremesti A, Paris F, Grassme H, Holler N, Tschopp J, Fuks Z, Gulbins E, Kolesnick R (2001) Ceramide enables fas to cap and kill. *J Biol Chem* **276:** 23954–23961

Dhein J, Daniel PT, Trauth BC, Oehm A, Moller P, Krammer PH (1992) Induction of apoptosis by monoclonal antibody anti-APO-1 class switch variants is dependent on cross-linking of APO-1 cell surface antigens. *J Immunol* **149:** 3166–3173

Di Guglielmo GM, Baass PC, Ou WJ, Posner BI, Bergeron JJ (1994) Compartmentalization of SHC, GRB2 and mSOS, and hyperphosphorylation of Raf-1 by EGF but not insulin in liver parenchyma. *EMBO J* **13:** 4269–4277

Eramo A, Sargiacomo M, Ricci-Vitiani L, Todaro M, Stassi G, Messina CG, Parolini I, Lotti F, Sette G, Peschle C, De Maria R (2004) CD95 death-inducing signaling complex formation and internalization occur in lipid rafts of type I and type II cells. *Eur J Immunol* **34:** 1930–1940

Gomez-Angelats M, Cidlowski JA (2003) Molecular evidence for the nuclear localization of FADD. *Cell Death Differ* **10:** 791–797

Grassme H, Jekle A, Riehle A, Schwarz H, Berger J, Sandhoff K, Kolesnick R, Gulbins E (2001) CD95 signaling via ceramide-rich membrane rafts. *J Biol Chem* **276:** 20589–20596

Huang DC, Tschopp J, Strasser A (2000) Bcl-2 does not inhibit cell death induced by the physiological Fas ligand: implications for the existence of type I and type II cells. *Cell Death Differ* **7:** 754–755

Itoh N, Nagata S (1993) A novel protein domain required for apoptosis. Mutational analysis of human Fas antigen. *J Biol Chem* **268:** 10932–10937

Kischkel FC, Hellbardt S, Behrmann I, Germer M, Pawlita M, Krammer PH, Peter ME (1995) Cytotoxicity-dependent APO-1 (Fas/CD95)-associated proteins form a death-inducing signaling complex (DISC) with the receptor. *EMBO J* **14:** 5579–5588

Legler DF, Micheau O, Doucey MA, Tschopp J, Bron C (2003) Recruitment of TNF receptor 1 to lipid rafts is essential for TNFalpha-mediated NF-kappaB activation. *Immunity* **18:** 655–664

Li-Weber M, Krammer PH (2003) Function and regulation of the CD95 (APO-1/Fas) ligand in the immune system. *Semin Immunol* **15:** 145–157

Martin DA, Siegel RM, Zheng L, Lenardo MJ (1998) Membrane oligomerization and cleavage activates the caspase-8 (FLICE/MACHalpha1) death signal. *J Biol Chem* **273:** 4345–4349

Martin DA, Zheng L, Siegel RM, Huang B, Fisher GH, Wang J, Jackson CE, Puck JM, Dale J, Straus SE, Peter ME, Krammer PH, Fesik S, Lenardo MJ (1999) Defective CD95/APO-1/Fas signal complex formation in the human autoimmune lymphoproliferative syndrome, type Ia. *Proc Natl Acad Sci USA* **96:** 4552–4557

Martin TF (2001) PI(4,5)P(2) regulation of surface membrane traffic. *Curr Opin Cell Biol* **13:** 493–499

Miaczynska M, Christoforidis S, Giner A, Shevchenko A, Uttenweiler-Joseph S, Habermann B, Wilm M, Parton RG, Zerial M (2004a) APPL proteins link Rab5 to nuclear signal transduction via an endosomal compartment. *Cell* **116:** 445–456

Miaczynska M, Pelkmans L, Zerial M (2004b) Not just a sink: endosomes in control of signal transduction. *Curr Opin Cell Biol* **16:** 400–406

Micheau O, Tschopp J (2003) Induction of TNF receptor I-mediated apoptosis via two sequential signaling complexes. *Cell* **114:** 181–190

Miyaji M, Jin ZX, Yamaoka S, Amakawa R, Fukuhara S, Sato SB, Kobayashi T, Domae N, Mimori T, Bloom ET, Okazaki T, Umehara H (2005) Role of membrane sphingomyelin and ceramide in platform formation for Fas-mediated apoptosis. *J Exp Med* **202:** 249–259

Motley A, Bright NA, Seaman MN, Robinson MS (2003) Clathrin-mediated endocytosis in AP-2-depleted cells. *J Cell Biol* **162:** 909–918

Muppidi JR, Siegel RM (2004) Ligand-independent redistribution of Fas (CD95) into lipid rafts mediates clonotypic T cell death. *Nat Immunol* **5:** 182–189

Nagata S (1999) Fas ligand-induced apoptosis. *Annu Rev Genet* **33:** 29–55

O'Reilly LA, Divisekera U, Newton K, Scalzo K, Kataoka T, Puthalakath H, Ito M, Huang DC, Strasser A (2004) Modifications and intracellular trafficking of FADD/MORT1 and caspase-8 after stimulation of T lymphocytes. *Cell Death Differ* **11:** 724–736

Oehm A, Behrmann I, Falk W, Pawlita M, Maier G, Klas C, Li-Weber M, Richards S, Dhein J, Trauth BC, Ponstingl H, Krammer PH (1992) Purification and molecular cloning of the APO-1 cell surface antigen, a member of the tumor necrosis factor/nerve growth factor receptor superfamily. Sequence identity with the Fas antigen. *J Biol Chem* **267:** 10709–10715

Ohno H, Stewart J, Fournier MC, Bosshart H, Rhee I, Miyatake S, Saito T, Gallusser A, Kirchhausen T, Bonifacino JS (1995) Interaction of tyrosine-based sorting signals with clathrin-associated proteins. *Science* **269:** 1872–1875

Perez D, White E (1998) E1B 19K inhibits Fas-mediated apoptosis through FADD-dependent sequestration of FLICE. *J Cell Biol* **141:** 1255–1266

Peter ME, Krammer PH (2003) The CD95(APO-1/Fas) DISC and beyond. *Cell Death Differ* **10:** 26–35

Peter ME, Legembre P, Barnhart BC (2005) Does CD95 have tumor promoting activities? *Biochim Biophys Acta* **1755:** 25–36

Qin Y, Camoretti-Mercado B, Blokh L, Long CG, Ko FD, Hamann KJ (2002) Fas resistance of leukemic eosinophils is due to activation of NF-kappa B by Fas ligation. *J Immunol* **169:** 3536–3544

Raucher D, Stauffer T, Chen W, Shen K, Guo S, York JD, Sheetz MP, Meyer T (2000) Phosphatidylinositol 4,5-bisphosphate functions as a second messenger that regulates cytoskeleton-plasma membrane adhesion. *Cell* **100:** 221–228

Schneider-Brachert W, Tchikov V, Neumeyer J, Jakob M, Winoto-Morbach S, Held-Feindt J, Heinrich M, Merkel O, Ehrenschwender M, Adam D, Mentlein R, Kabelitz D, Schutze S (2004) Compartmentalization of TNF receptor 1 signaling; internalized TNF receptosomes as death signaling vesicles. *Immunity* **21:** 415–428

Screaton RA, Kiessling S, Sansom OJ, Millar CB, Maddison K, Bird A, Clarke AR, Frisch SM (2003) Fas-associated death domain protein interacts with methyl-CpG binding domain protein 4: a potential link between genome surveillance and apoptosis. *Proc Natl Acad Sci USA* **100:** 5211–5216

Shenoy-Scaria AM, Gauen LK, Kwong J, Shaw AS, Lublin DM (1993) Palmitylation of an amino-terminal cysteine motif of protein tyrosine kinases p56lck and p59fyn mediates interaction with glycosyl-phosphatidylinositol-anchored proteins. *Mol Cell Biol* **13:** 6385–6392

Shimizu S, Eguchi Y, Kamiike W, Waguri S, Uchiyama Y, Matsuda H, Tsujimoto Y (1996) Bcl-2 blocks loss of mitochondrial membrane potential while ICE inhibitors act at a different step during inhibition of death induced by respiratory chain inhibitors. *Oncogene* **13:** 21–29

Siegel RM, Frederiksen JK, Zacharias DA, Chan FK, Johnson M, Lynch D, Tsien RY, Lenardo MJ (2000) Fas preassociation required for apoptosis signaling and dominant inhibition by pathogenic mutations. *Science* **288:** 2354–2357

Siegel RM, Muppidi JR, Sarker M, Lobito A, Jen M, Martin D, Straus SE, Lenardo MJ (2004) SPOTS: signaling protein oligomeric transduction structures are early mediators of death receptor-induced apoptosis at the plasma membrane. *J Cell Biol* **167:** 735–744

Stegh AH, Barnhart BC, Volkland J, Algeciras-Schimnich A, Ke N, Reed JC, Peter ME (2002) Inactivation of caspase-8 on mitochon-

dria of Bcl-xL-expressing MCF7-Fas cells: role for the bifunctional apoptosis regulator protein. *J Biol Chem* **277:** 4351–4360

Stolz LE, Huynh CV, Thorner J, York JD (1998) Identification and characterization of an essential family of inositol polyphosphate 5-phosphatases (INP51, INP52 and INP53 gene products) in the yeast *Saccharomyces cerevisiae*. *Genetics* **148:** 1715–1729

Tanaka M, Itai T, Adachi M, Nagata S (1998) Downregulation of Fas ligand by shedding. *Nat Med* **4:** 31–36

Teis D, Wunderlich W, Huber LA (2002) Localization of the MP1–MAPK scaffold complex to endosomes is mediated by p14 and required for signal transduction. *Dev Cell* **3:** 803–814

Wunderlich W, Fialka I, Teis D, Alpi A, Pfeifer A, Parton RG, Lottspeich F, Huber LA (2001) A novel 14-kilodalton protein interacts with the mitogen-activated protein kinase scaffold mp1 on a late endosomal/lysosomal compartment. *J Cell Biol* **152:** 765–776